

RESEARCH PAPER

Biochemical and pharmacological characterization of nuclear urotensin-II binding sites in rat heart

ND Doan^{1,2*}, TTM Nguyen^{1,2*}, M Létourneau^{1,2}, K Turcotte^{1,2},
A Fournier^{1,2} and D Chatenet^{1,2}

¹Laboratoire d'études moléculaires et pharmacologiques des peptides, Université du Québec, INRS – Institut Armand-Frappier, Ville de Laval, QC, Canada, and ²Laboratoire International Associé Samuel de Champlain (INSERM – INRS – Université de Rouen), Ville de Laval, QC, Canada

Correspondence

Dr Alain Fournier, Laboratoire d'études moléculaires et pharmacologiques des peptides, Université du Québec, INRS – Institut Armand-Frappier, 531 Boulevard des Prairies, Ville de Laval, QC, Canada H7V 1B7.
E-mail: alain.fournier@iaf.inrs.ca

*Both authors contributed equally to the work.

Keywords

urotensin-II; urotensin II-related peptide; nuclear receptors; intracrine; cardiovascular; endocytosis

Received

21 March 2011

Revised

12 August 2011

Accepted

17 September 2011

BACKGROUND AND PURPOSE

During the past decade, a few GPCRs have been characterized at the nuclear membrane where they exert complementary physiological functions. In this study, we investigated (1) the presence of a functional urotensin-II (U-II) receptor (UT) in rat heart nuclear extracts and (2) the propensity of U-II and U-II-related peptide (URP) to cross the plasma membrane in a receptor-independent manner.

EXPERIMENTAL APPROACH

Biochemical and pharmacological methods including competitive binding assays, photoaffinity labelling, immunoblotting as well as *de novo* RNA synthesis were used to characterize the presence of functional UT receptors in rat heart nuclei. In addition, confocal microscopy and flow cytometry analysis were used to investigate the cellular uptake of fluorescent U-II and URP derivatives.

KEY RESULTS

The presence of specific U-II binding sites was demonstrated in rat heart nuclear extracts. Moreover, such subcellular localization was also observed in monkey heart extracts. *In vitro* transcription initiation assays on rat, freshly isolated, heart nuclei suggested that nuclear UT receptors are functional, and that U-II, but not URP, participates in nuclear UT-associated gene expression. Surprisingly, hU-II and URP efficiently crossed the plasma membrane in a receptor-independent mechanism involving endocytosis through caveolin-coated pits; this uptake of hU-II, but not that of URP, was dependent on extracellular pH.

CONCLUSION

Our results suggest that (1) U-II and URP can differentially modulate nuclear UT functions such as gene expression, and (2) both ligands can reach the internal cellular space through a receptor-independent mechanism.

Abbreviations

Ahx, L-2-aminohexanoic acid; BOP, benzotriazol-1-yl-oxy-*tris*(dimethylamino)-phosphonium hexafluorophosphate; Bpa, *para*-benzoyl-phenylalanine; DCM, dichloromethane; DIEA, *N,N*-diisopropylethylamine; DMF, dimethylformamide; FITC, fluorescein isothiocyanate; MALDI-TOF, matrix-assisted laser desorption/ionization – time-of-flight; MEM, minimum essential medium; MFI, mean fluorescence intensity; Nup62, nucleoporin 62; PACAP(28-38), C-terminal segment 28–38 of pituitary adenylate cyclase-activating polypeptide; PTX, pertussis toxin; TFA, trifluoroacetic acid; U-II, urotensin-II; URP, urotensin-II-related peptide; UT, urotensin-II receptor

Introduction

Urotensin-II (U-II), initially isolated from the teleost urophysis, was later found to be also expressed in mammals where it was characterized as a potent vasoconstrictor (Vaudry *et al.*, 2010). While all U-II isoforms contain a conserved C-terminal cyclic hexapeptide, the N-terminal segment is highly variable (Leprince *et al.*, 2008). A paralogue peptide, the U-II-related peptide (URP), was isolated from rat brain extracts, and mature forms from other mammalian species, including humans, were predicted from prepro-URP cDNA sequences (Sugo and Mori, 2008). So far, all mammalian URP isoforms are strictly identical (Leprince *et al.*, 2008). Structurally related, U-II and URP possess the conserved cyclic region encompassing the biologically active triad Trp-Lys-Tyr (Leprince *et al.*, 2008). Both peptides are endogenous ligands of a GPCR known as UT, belonging to subclass 1A of GPCRs (Lavecchia *et al.*, 2005; Proulx *et al.*, 2008). The urotensinergic system is not only widely distributed within the CNS but also in the peripheral nervous system and more precisely within the cardiovascular system where it exerts inotropic effects, vascular smooth muscle cell proliferation, remodelling changes as well as vasoconstriction or vasodilatation depending on the vascular bed (Dubessy *et al.*, 2008; Russell, 2008). Because U-II was isolated more than 10 years before its peptide paralogue, it has always been considered as the peptide of interest, and most of the *in vitro* and *in vivo* studies are related to its putative effects and pathophysiological relevance. In fact, a high expression of U-II and its receptor has been found to be associated with several pathological states including hypertension, atherosclerosis, heart failure, pulmonary hypertension, diabetes mellitus and renal failure (Ross *et al.*, 2010).

Once bound to its receptor, U-II gives rise to the generation of second messengers (i.e. inositol triphosphate and diacylglycerol), leading to intracellular calcium release and activation of different pathway systems such as p38MAPK, ERK1/2 and Rho A/ROCK (Proulx *et al.*, 2008). However, the intracellular signalling of URP has not been thoroughly studied, most probably because of its structural homology with U-II and similar potencies at triggering calcium release in UT-transfected cells (Dubessy *et al.*, 2008) and inducing hypotension in anaesthetized rats (Sugo and Mori, 2008). However, the differential distribution of U-II and URP mRNAs suggests that these peptides could have complementary biological functions (Vaudry *et al.*, 2010). Corroborating this assertion, two studies have demonstrated that these two peptides exert different biological effects on astrocyte cell proliferation (Jarry *et al.*, 2010) and cardiac contractility (Prosser *et al.*, 2008).

In many species, including chicken, rodent and human, it has been shown that the U-II gene is closely related to the cortistatin gene, whereas the URP gene is located on the same chromosome as somatostatin (Tostivint *et al.*, 2008). Interestingly, cortistatin shares many biological activities with somatostatin and is not only able to bind and activate all its receptors but also possesses unique functional activities (Ferone *et al.*, 2006). An undiscovered receptor subclass and/or a receptor dimerization (homo or hetero) phenomenon could explain this kind of atypical pharmacological profile. Nevertheless, an increasing amount of evidence

shows that the localization of GPCRs is not limited to the plasma membrane, and that functional GPCRs can be found at the nuclear membrane. In particular, functional β -adrenergic, endothelin and angiotensin receptors were characterized at the cell nucleus (Boivin *et al.*, 2006). Moreover, it has been suggested that these intracellular receptors can trigger different signalling pathways in relation to their localization (Vaniotis *et al.*, 2011).

In this study, we investigated the presence of functional UT receptors on the nuclear membrane and probed the ability of both endogenous ligands (i.e. U-II and URP) to cross the plasma membrane. Our results demonstrated the propensity of both peptides to enter, in a receptor-independent manner, the intimal compartment and to differentially activate the receptor found in nuclei extracted from the rat heart. This study establishes the presence of functionally coupled UT receptors in nuclei isolated from heart tissue and raises the question about its physiological and pathophysiological role upon U-II and/or URP activation.

Methods

Materials

Fmoc-protected amino acids, Wang polystyrene resin and BOP reagent [benzotriazol-1-yl-oxy-tris(dimethylamino)-phosphonium hexafluorophosphate] were purchased from Chem-Impex (Wood Dale, IL, USA). Common solvents for solid phase peptide synthesis and purification were obtained from Fisher Scientific (Nepean, ON, Canada), whereas trifluoroacetic acid (TFA) was from PSIG (Montreal, QC, Canada). Isotopes (i.e. Na¹²⁵I and ³²P-labelled uracil) were purchased from Perkin Elmer (Montreal, QC, Canada). Anti-fade reagent (ProLong), streptavidin-Alexa Fluor 568 conjugate, Alexa Fluor 448 conjugated anti-rabbit and Alexa Fluor 568 conjugated anti-mouse secondary antibodies as well as dNTPs were supplied by Invitrogen (Burlington, ON, Canada). Other chemicals, including chloramine-T, sodium bisulfite, nocodazole, nystatin, amiloride, sucrose, pertussis toxin (PTX), ammonium chloride, chloroquine, maleimide, sodium azide, fluorescein isothiocyanate (FITC), D-biotin, propidium iodide (PI), bacitracin, iodoacetamide, dithiothreitol (DTT), PMSF, the protease inhibitor cocktail, secondary antibodies as well as cell culture media and additives were ordered from Sigma Aldrich (Mississauga, ON, Canada). Rabbit anti-UT receptor antibodies were from GeneTex (San Antonio, TX) or from Alpha diagnostic International (San Antonio, TX), whereas rabbit anti-nucleoporin 62, anti-caveolin-3, anti-cytochrome C and anti-lamin A antibodies were purchased from Santa Cruz Biotechnology (Santa Cruz, CA, USA). DRAQ5TM nuclear staining reagent was from Biossatus Ltd. (Leicestershire, UK). The biotinylated anti-rabbit secondary antibody was obtained from Vector Laboratories (Burlington, ON, Canada). SuperSignal West Pico chemoluminescent substrate and monomeric avidin columns were from Pierce Biotechnology (Rockford, IL, USA), while the Nuclear Extract kit was from Active Motif (Carlsbad, CA, USA). The DC Protein Assay kit, used for protein quantification, and PVDF membranes were purchased from Bio-Rad (Montreal, QC, Canada).

Peptide synthesis

Human (h) and rat U-II, URP, N-biotin-[Ahx⁰, Bpa³]-hU-II, TAT(48–60) and PACAP(28–38), as well as their fluorescent derivatives, were synthesized using Fmoc chemistry with a BOP coupling strategy as previously described (Brkovic *et al.*, 2003). In order to obtain FITC-conjugated peptides, peptidyl resins were coupled with an ϵ -amino acid (Fmoc-Ahx-OH) and then were reacted overnight with FITC (1.2 equiv) and triethylamine (20 equiv) in a DMF/DCM mixture (1:1) (Jullian *et al.*, 2009). TFA-mediated cleavage (TFA/ethanedithiol/phenol/water; 92/2.5/3/2.5; 2 h) afforded the expected fluorescent peptides. Cyclization of hU-II, URP and their fluorescent analogues (FL-hU-II and FL-URP) was mediated by iodine (10% in methanol) in a mixture of acetic acid (70% in water) for 30 min and stopped by the addition of ascorbic acid (Erchegeyi *et al.*, 2005). Preparative RP-HPLC was carried out using a Phenomenex Luna C₁₈ column (250 × 21.2 mm), and fractions were analysed using matrix-assisted laser desorption/ionization – time-of-flight (MALDI-TOF) mass spectrometry (Voyager DE system from Applied Biosystems in linear mode using the α -cyano-4-hydroxycinnamic acid matrix, Carlsbad, CA, USA) and analytical RP-HPLC with a Phenomenex Jupiter C₁₈ column (250 × 2.4 mm). Fractions corresponding to the desired product with purity greater than 98% were pooled and lyophilized. The physicochemical characteristics of all peptides are shown in Figure S1 (see supporting information).

Calcium mobilization assay

Activation of UT receptors was evaluated with a functional cell line co-expressing human UT receptors and a mitochondrial apo-aequorin protein from Euroscreen in accordance with the manufacturer's protocol (Gosselies, Belgium). A detailed experimental procedure is provided in the supporting information (Appendix S1).

Peptide iodination

Synthetic hU-II, URP and N-biotin-[Ahx⁰, Bpa³]-hU-II were radiolabelled with 0.5 mCi Na¹²⁵I using the chloramine-T technique, as previously described (Doan *et al.*, 2011). Iodinated peptides were purified using a C₁₈ Sep-Pak cartridge (Waters Corp., Milford, MA, USA), collected and stored at –20°C until use.

Nuclear receptor binding assay

Radioligand binding assays were performed with 150 μ g of proteins in a binding buffer containing 50 mM Tris-base (pH 7.4), 100 mM NaCl, 10 mM MgCl₂, 0.1% BSA, 1 mM PMSF for a reaction volume of 500 μ L. For competition studies, 0.2 nM [¹²⁵I]-hU-II was incubated with unlabelled hU-II, URP, urantide or somatostatin (10^{–6} M). After a 2 h incubation, the reaction was stopped by rapid filtration under reduced pressure through Whatman glass microfibre filters (GF/C) pre-soaked in 5% skim milk with a 1225 Sampling Manifold from Millipore (Bedford, MA, USA). Filters were rinsed three times with cold 25 mM Tris-HCl (pH 7.5) and then counted using a γ -counter to quantify residual radioactivity. Data were plotted in a displacement histogram using Prism 4.0 (GraphPad Software, San Diego, CA, USA).

Protein isolation

Male Sprague–Dawley rats (200–250 g) were obtained from Charles River (St-Constant, QC, Canada). All experiments were performed according to the recommendations of the ethics committee of this research centre and were supervised by authorized investigators. First, rats were killed by carbon dioxide asphyxiation, and then fresh heart tissues were isolated and placed in cold PBS. Hearts from male cynomolgus monkeys were a generous gift from Pr. Veronika von Messling (INRS-IAF, Laval, QC, Canada). Tissues were weighed, diced, pulverized in liquid nitrogen to obtain a fine powder and finally homogenized with a Polytron. Whole cell and nuclear proteins were isolated according to the supplier's procedure described in the Nuclear Protein Extract kit. Protein samples were quantified following the Bio-Rad DC Protein Assay.

Isolation of membrane and nuclei from heart

A procedure described by Boivin *et al.* (2003) was followed. The nuclei enriched pellet was re-suspended and stored at –80°C until use or directly re-suspended in transcription buffer for transcription initiation assay (Appendix S1).

Electrophoresis and immunoblotting

Protein extracts were separated either by 1D- or 2D-PAGE. Experimental details are presented in the supporting information (Appendix S1).

Purification and characterization of photolabelled complexes

Transfected CHO cells overexpressing the UT receptor were used as a positive control for the photolabelling and purification processes applied to membrane preparations and nuclei isolated from rat heart tissues. Radiolabelled N-biotin-[Ahx⁰, Bpa³]-hU-II (5 nM) was incubated for 90 min at room temperature with 200 μ g of proteins from either rat heart (whole nuclei or enriched membrane fraction) or CHO-UT transfected cells (Chatenet *et al.*, 2004) in a buffer composed of 50 mM Tris-HCl (pH 7.4), 100 mM NaCl, 10 mM MgCl₂, 0.1% (w/v) BSA, 1 mM PMSF and 0.01% (v/v) of protease inhibitor cocktail. Then, the total volume (200 μ L) was transferred into a Millipore-Microcon centrifugal device (molecular cut-off: 10 kDa), which was used in accordance with the manufacturer's recommendations to remove unbound peptide. Resulting peptide–protein complexes were washed four times with 500 μ L of binding buffer in these centrifugal devices before being transferred to a well of 96-well plate placed on ice. Volumes were adjusted to 100 μ L, and samples were irradiated for 1 h with a UV lamp (100 W, 365 nm) in order to activate the Bpa residue of the U-II analogue and to obtain a covalent bond between the biotinylated peptide probe and the bound protein. Proteins were solubilized by adding 150 μ L of a lysis buffer [50 mM Tris-HCl (pH 8.0), 150 mM NaCl, 0.5% (v/v) Igepal, 0.1% (w/v) SDS, 0.1% (v/v) Triton X-100 and 0.1% (v/v) of the protease inhibitor cocktail] to each well. Following a 30 min incubation at 4°C, insoluble proteins were removed by centrifugation (45 min, 13 000 \times g, 4°C). Supernatants were kept for purification of the biotinylated photolabelled complex with monomeric avidin columns from Pierce. As recommended by the manufacturer, columns were treated with a 2 mM D-biotin/PBS solution to block irreversible binding sites,

regenerated with a 100 mM glycine-HCl buffer (pH 2.8) and washed four times with PBS. Proteins to be purified (150 µg) were loaded onto the column along with 1.8 mL of PBS and let to stand for 1 h at room temperature. Then, the column was washed four times with PBS and eluted with 2 mM D-biotin/PBS. Specifically bound photolabelled complexes were collected as 2 mL fractions and counted with a γ counter. Fractions with the highest radioactivity counts were lyophilized and kept at -20°C until further use. The photolabelled receptors were solubilized in water and then analysed using a 10% SDS-PAGE performed during 2 h at 100 V. Gels were dried on a cellophane membrane and revealed onto an X-ray film, in the presence of an intensifying screen.

Transcription initiation assay

Transcription initiation was evaluated in freshly isolated nuclei from rat heart, as previously described with small modifications to the protocol (Boivin *et al.*, 2006); a detailed description is provided in the supporting information (Appendix S1).

Binding assay

The presence of specific binding sites at the cellular membrane was assessed by competitive binding assays performed on CHO-K1, HEK-293 and HeLa cells. Cells were seeded at a density of 500 000 cells per well in six-well plates and cultured at 37°C in a humidified atmosphere of 5% CO_2 and 95% air. After 24 h, medium was removed, and cells were washed three times with binding buffer [25 mM Tris-HCl, 25 mM MgCl_2 , 1% (w/v) BSA, and $5\ \mu\text{g}\cdot\text{L}^{-1}$ bacitracin] and then exposed to 0.2 nM of [^{125}I]-hU-II or [^{125}I]-URP in the presence or not of hU-II or URP (10^{-5} M), respectively. Following a 2 h incubation at room temperature, cells were washed twice, lysed with NaOH (0.1 M), and the cell-bound radioactivity was quantified using a γ -counter (1470 Automatic Gamma Counter, Perkin Elmer).

Confocal microscopy

To monitor receptor-independent uptake, CHO-K1, HeLa and HEK-293 cells were plated on an eight-well chamber slide (Lab-Tek, Nalge Nunc International, Rochester, NY, USA) and incubated for 24 h at 37°C in a humidified atmosphere of 5% CO_2 and 95% air. Subcellular localization was assessed by incubating adherent cells with fluorescent peptides (FL-hU-II and FL-URP, 10^{-6} M) for 1 h at 37°C in HEPES-Krebs-Ringer (HKR) buffer (5 mM HEPES, 137 mM NaCl, 2.68 mM KCl, 2.05 mM MgCl_2 , 1.8 mM CaCl_2 and $1\ \text{g}\cdot\text{L}^{-1}$ glucose, pH 7.4) (Holm *et al.*, 2006). Following careful washes with an acidic aqueous solution containing 0.2 M glycine and 0.1 M NaCl (pH 4) and then PBS, cell nuclei were stained with DRAQ5TM (5 µM) for 15 min. For HeLa cells, an additional staining step was added before the nuclear staining. Following incubation with fluorescent peptides and acid washes, non-specific binding was blocked with 10% goat serum in PBS for 1 h at room temperature. Cells were then incubated with anti-caveolin-3 primary antibody (1:200) at 4°C overnight. Coverslips were washed several times with PBS and incubated with a biotinylated anti-rabbit secondary antibody (1:200) for 1 h at room temperature. Unbound secondary antibodies were removed by washing, and cells were then incubated

with $1\ \mu\text{g}\cdot\text{mL}^{-1}$ of Streptavidin-Alexa Fluor 568 conjugate in PBS for another hour. The peptide subcellular localization was directly analysed with an oil immersion Nikon Plan Apo 100 objective mounted onto a Nikon Eclipse E800 microscope (Nikon, Melville, NY, USA) equipped with a Bio-Rad Radiance 2000 confocal imaging system (Bio-Rad Laboratories, Hercules, CA, USA).

For studies using pharmacological inhibitors, living CHO-K1 cells were pre-incubated, for 30 min at 37°C , with one of the following agents: nocodazole (20 µM), nystatin ($25\ \mu\text{g}\cdot\text{mL}^{-1}$), sucrose (0.25 M) or amiloride (2.5 mM). Other inhibitors such as NH_4Cl (10 mM), chloroquine (50 µM) and maleimide (10 µM) were introduced into the culture medium (without FBS) 10 min before FITC-labelled peptide treatment (10^{-6} M). Finally, PTX, a $\text{G}_{i/o}$ -protein blocker, was added ($200\ \text{ng}\cdot\text{mL}^{-1}$) to cells in serum-free medium 6 h before addition of the fluorescent peptides (10^{-6} M).

In order to evaluate the effect of low temperature on the cellular uptake, CHO-K1 cells were cooled to 4°C in serum-free medium 15 min before the incubation with fluorescent peptides (10^{-6} M) and maintained at this temperature for 1 h. It should be noted that all solutions were also cooled to 4°C before use.

Left ventricles from rat heart tissue were isolated, fast frozen, sliced into serial 6 µm-thick sections and mounted on slides. Frozen sections were fixed in methanol : acetone (1:1) for 10 min at room temperature and then rehydrated with 100% ethanol (5 min, 3 times) and 95% ethanol (1 min) respectively. Slides were incubated for 45 min at room temperature in a blocking buffer containing 1% BSA, 10% goat serum and 0.1% Triton X-100 in PBS. Double labelling was performed by incubating sections in PBS (1% BSA) containing rabbit anti-rat UT (1:50) and mouse anti-lamin A (a protein related to inner nuclear envelope; 1:50) for 2 h at room temperature. Secondary antibodies (i.e. Alexa Fluor 488-conjugated anti rabbit and Alexa Fluor 568-conjugated anti mouse) were diluted (1:2000 each) in PBS containing 5% goat serum and then applied to the slides for 1 h at RT. After each incubation, sections were rinsed with PBS at least three times. Nuclei were stained for 15 min at room temperature with DRAQ 5 (5 µM). After the final washing with PBS, the sections were air-dried and then mounted with ProLong to prevent photobleaching. Negative controls (i.e. non-specific binding of the secondary antibodies obtained by omitting primary antibodies in the staining protocol) were included for each experiment. Microscopic analysis was performed with the confocal microscope described above.

Flow cytometry

As previously mentioned, cell lines lacking UT receptors were used to monitor receptor-independent uptake. Cells seeded in 12-well plates were incubated with fluorescent peptides as described for confocal microscopy. After acid washes to remove unbound and surface-bound ligand, cells were then enzymatically removed from the surface with trypsin/EDTA (5 min at 37°C), and the reaction was quenched by adding 10% FBS/PBS. After centrifugation (5 min at $1000\times g$), pelleted cells were re-suspended in 500 µL of PBS containing $0.5\ \mu\text{g}\cdot\text{mL}^{-1}$ of PI and kept on ice until analysis. A minimum of 10 000 cells per sample were then analysed on a FACScan (BD Biosciences, San Jose, CA, USA). PI staining positive cells

were excluded from the analysis, and the mean fluorescence intensity (MFI) of the living cell population was used for statistical analysis. Data interpretation was achieved with WinMDI software (Windows Multiple Document Interface for Flow Cytometry).

Kinetics of entry was investigated by incubating CHO-K1 cells with FITC-conjugated peptides (10^{-6} M) for various periods of time at 37°C in HKR buffer while following the protocol described above. Maximal uptake was calculated as the amount of internalized peptide at 37°C after 1 h.

To study the effect of pH on the cellular uptake of FL-hU-II and FL-URP, an HKR buffer for which the pH was adjusted at 6.5, 7.0, 7.5 and 8.0 was used following the same protocol.

Experiments investigating the effects of pharmacological inhibitors or of temperature on uptake were performed as described in the confocal microscopy section, except that DRAQ5™ was replaced with PI.

Data analysis

Data are expressed as mean \pm SEM. Statistical analysis was assessed using Prism version 4.0 (GraphPad) with a one-way ANOVA followed by a Dunnett's post-test, a two-way ANOVA followed by a Bonferroni's post-test or Student's unpaired *t*-test.

Results

Identification and biochemical characterization of nuclear U-II binding sites

A biotinylated photoactivable peptide probe, N-biotin-[Ahx⁰, Bpa³]hU-II, was used to pull down U-II binding sites from nuclear proteins. The identity of the derivative was assessed by mass spectrometry and RP-HPLC, and the probe was found to have a similar calcium mobilization potency and efficacy as that of hU-II (see Figure S1). Photolabelled complexes, obtained with radiolabelled N-biotin-[Ahx⁰, Bpa³]-

hU-II and three different preparations, that is, CHO-UT transfected cells (positive control), as well as membrane and nuclear heart extracts were isolated on a column of monomeric avidin and migrated on SDS-PAGE (Figure 1A). Nuclear heart extracts were characterized by verifying the presence of specific known subcellular marker proteins including caveolin-3 (rafts-plasma membrane), cytochrome C (mitochondria) and Nup62 (nuclear envelope) (Figure 1A). Immunoreactivity against UT and Nup62, but not for caveolin-3 and cytochrome C, was detected in the nuclear fraction, demonstrating the high purity of this nuclear extract. The results from the photolabelling experiments showed the presence of only one protein specifically and covalently labelled

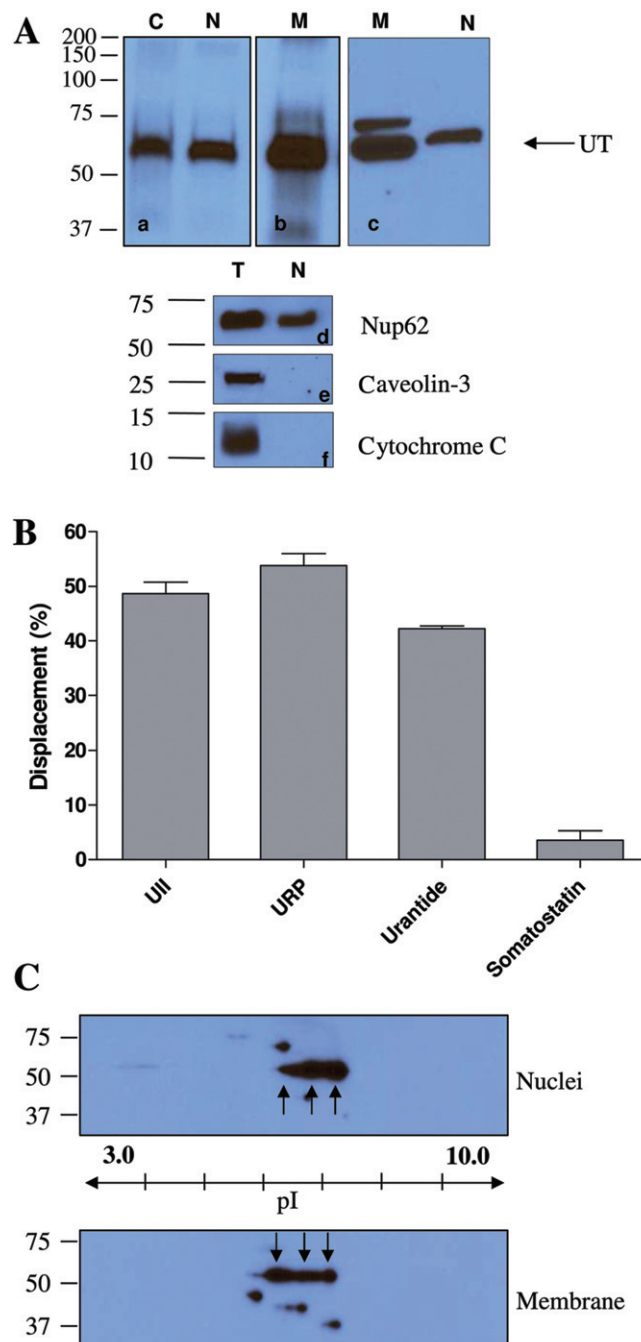


Figure 1

(A) Purified photolabelled complexes from CHO-UT total protein, rat heart nuclear extracts and rat heart membrane proteins characterized by autoradiography (a,b). UT detection in rat heart extracts by immunoblotting using GeneTex anti-UT antibody (c). C: total proteins from CHO-UT transfected cells (positive control), N: rat heart nuclear extracts and M: rat heart membrane proteins extract, T: rat heart total proteins. Proteins isolated from rat heart tissues were resolved using 10% SDS-PAGE and analysed by Western blot using anti-Nup62 (d), anti-caveolin 3 (e) and anti-cytochrome C (f) as described in the experimental section. (B) [¹²⁵I]-hU-II binding to rat isolated heart nuclei and displacement by non-radioactive peptides. Results shown are the amount of bound [¹²⁵I]-hU-II displaced when incubated in the presence of the unlabelled peptide indicated. Data are mean \pm SEM of at least three independent experiments, and each determination was performed in duplicate. (C) 2D immunoblots revealed with anti-UT antibody performed on membrane and nuclear proteins extracted from rat heart. Proteins were isoelectrically focused in a pH gradient of 3 to 10 and then resolved through a 10% SDS-PAGE as described in the Methods section. Immunoreactive species corresponding to the UT receptor are located between 50 and 75 kDa at a pI value of 6–7.

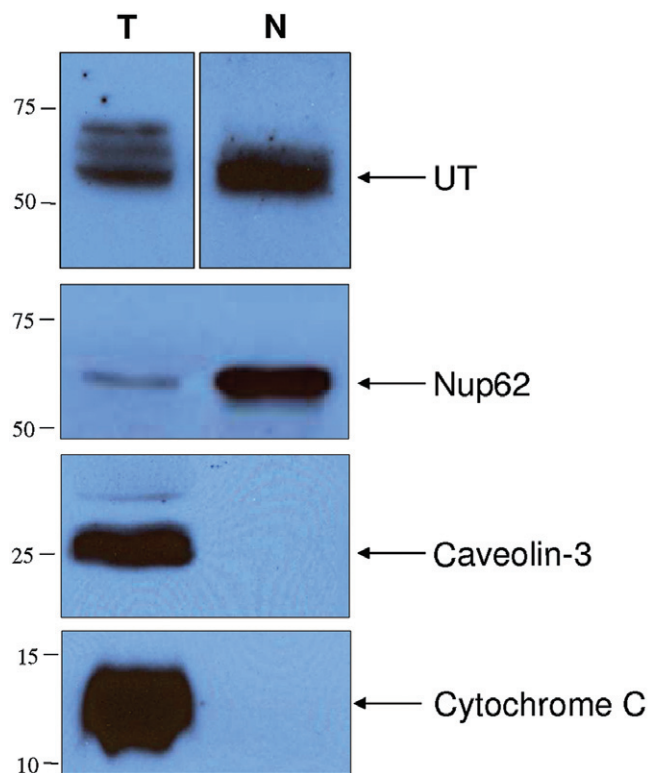


Figure 2

Total (T) and nuclear (N) protein extracts isolated from cynomolgus monkey heart. Total and nuclear proteins were resolved using 10% SDS-PAGE and analysed by Western blot using anti-Nup62, anti-caveolin 3 and anti-cytochrome C, as described in the Methods section.

with the U-II analogue in these three preparations (Figure 1A). Moreover, immunoblotting, using specific antisera against UT, also identified a band of ~60 kDa in the rat heart nuclear extract supporting the abovementioned results. Radioligand binding assays, performed on nuclei isolated from the rat heart, demonstrated the propensity of hU-II and URP to displace specifically bound radiolabelled hU-II (Figure 1B). Nuclear U-II binding sites were pharmacologically characterized using urantide, an UT-selective antagonist, and somatostatin, a peptide sharing sequence homology with the U-II peptides. Like U-II and URP, urantide was able to displace, in a similar manner, bound [125 I]-hU-II, whereas somatostatin was unable to displace it (Figure 1B). These observations suggest (1) that the receptor expressed in the isolated nuclei is probably the UT receptor, (2) that it specifically binds its cognate ligands and specific antagonist and (3) that it is not a somatostatin-like receptor.

Nuclear UT receptors were further characterized through 2D-PAGE immunoblotting. Nuclear and membrane proteins extracted from heart tissues expressed three major UT-immunoreactive spots with an apparent molecular weight of 60 kDa at a pI value of 6–7 (Figure 1C). Finally, UT receptors were also detected in the nuclear proteins extracted from cynomolgus monkey heart (Figure 2), showing that this subcellular localization is not restricted to rodents. Interestingly, the anti-UT antibody (GeneTex) used in Figures 1 and 2

was raised against a human C-terminal receptor fragment, and species cross-reactivity had not been tested by the manufacturer. Our results show that it also specifically recognizes rat UT receptors since the immunoreactive species detected in rat tissue preparations (Figure 1Ac) corresponded to the band observed with the photolabelling experiments (Figure 1Aa,Ab) and with Western blot results from cynomolgus monkey tissues (Figure 2).

Nuclear localization of the UT receptor by confocal microscopy

The subcellular localization of UT receptors was further studied in rat ventricular tissue section by confocal immunofluorescence microscopy using a rabbit anti-rat UT selective antibody (Alpha Diagnostic). Specificity of this antibody was previously demonstrated (Gong *et al.*, 2004). Of note, and as previously reported, no specific staining was observed in right ventricular sections (data not shown) (Gong *et al.*, 2004). Left ventricular sections were double-stained for UT and lamin A and imaged with confocal microscopy. Nuclei were counterstained with DRAQ5TM (Figure 3A,E). As expected, immunostaining associated to lamin A, a nuclear envelope protein, was mostly surrounding nuclei (Figure 3B), while the UT staining was more diffused (Figure 3C), probably reflecting the presence of receptors across cardiomyocyte cell membranes exposed on the tissue cryosection. Moreover, co-localization of UT and lamin A was observed under immunofluorescence double staining (Figure 3D), suggesting that UT might be localized at, or in the close vicinity of, the nuclear membrane. An enlargement of a nucleus can be found in the supporting information (Figure S2). Control experiments using only the secondary antibodies detected minimal non-specific fluorescence under the imaging conditions employed (Figure 3F–H).

Transcription initiation

Transcriptional activity of U-II isoforms and URP on rat heart isolated nuclei was assessed by *in vitro* transcription initiation assays (Figure 4). Purity of nuclei used for this assay is shown in Figure 1 and demonstrated no important contamination of membrane or mitochondrial protein. In addition, this fractionation protocol was previously shown to yield a negligible amount of endoplasmic reticulum elements (Boivin *et al.*, 2003). As shown, total transcription was increased in rU-II- and hU-II-, but not URP-, treated nuclei. Interestingly, a typical bell-shaped curve was observed with hU-II but not rU-II. Pretreatment of nuclei with urantide completely abolished the rU-II- and hU-II-associated transcriptional activity, while urantide alone was unable to stimulate transcription.

Cellular uptake of fluorescein-conjugated hU-II (FL-hU-II) and URP (FL-URP)

In these experiments, the well-established cell-penetrating peptide TAT(48–60) (Dennison *et al.*, 2007) and the PACAP(28–38) segment that has no cell-penetrating properties were used as positive and negative controls, respectively. It is important to mention that cell lines (CHO-K1, HeLa and HEK-293) used in those experiments are not known to endogenously express UT receptors. Moreover, the presence of UT receptors on these cell types was assessed through binding

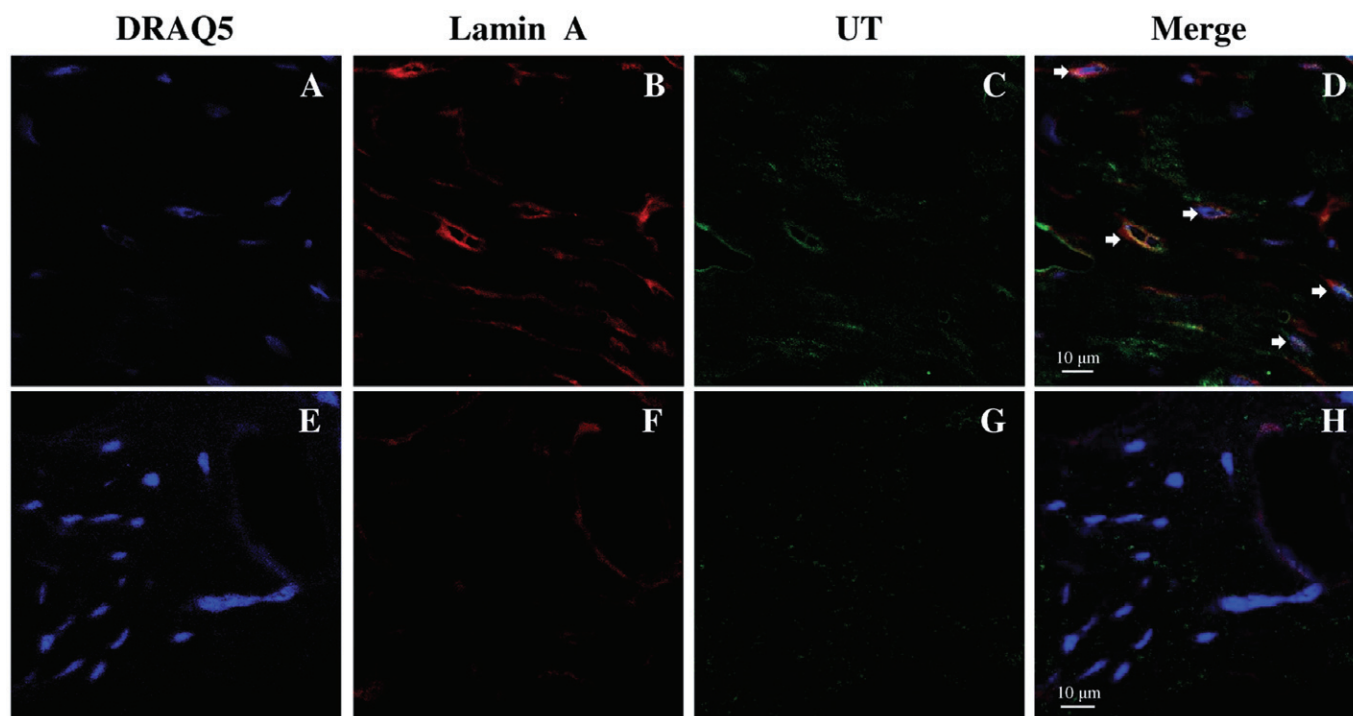


Figure 3

Immunofluorescence double staining with anti-UT and anti-lamin A antibodies show positive signals for UT protein on the cardiac myocytes imaged with a confocal microscope. Nuclei are stained with DRAQ5™ (A,E, blue signal). Left ventricular sections are double-stained for lamin A (B, red signal) and UT (C, green signal). (D) is the superimposition of (A), (B) and (C), showing the co-localization of UT (yellow signal, arrowhead) and the nuclear envelope. (F) and (G) represent negative control sections using 1% BSA-PBS instead of primary antibodies. (H) is the superimposition of (E), (F) and (G), showing no co-localization of the non-specific labelling.

experiments using ^{125}I -labelled peptides (0.2 nM) in the presence or not of cold peptide (10^{-6} M). As shown in Figure 5, no significant displacement was observed with either hU-II or URP (data presented in Figure 5 are representative of the CHO-K1 cells, but similar results were obtained with HEK-293 and HeLa cells). These results suggest that UT receptors are probably not present (or at a very low density) on the cellular membrane of these cell types. Using confocal microscopy analysis on fixed (Figure S3) or living (Figure 6A) CHO-K1 cells, we demonstrated the propensity of FL-hU-II and FL-URP to cross the plasma membrane in order to be located not only in the cytoplasm but also in the nucleus. However, for both peptides, the signal recorded at the nucleus in living cells was weak but still representative of a nuclear localization of the peptides. Similar distributions were also observed in other cell types such as HEK-293 and HeLa cells, demonstrating that hU-II and URP can enter into different cell types (see Figure S4). Interestingly, incubation with FL-URP resulted in a punctuate cytoplasmic distribution that may represent endocytic vesicles (Figure 6A).

Quantification of cellular uptake confirmed the ability of both peptides to efficiently penetrate inside the intracellular compartment but with a lower potency than TAT(48–60) (Figure 6B–D). Even if no uptake variation was observed between cell lines for FL-hU-II or FL-URP, a significant difference in the uptake between both peptides was observed in each cell line (Figure 6B). Both peptides were also shown to be

taken up by cells in a concentration-dependent manner, and a good uptake, represented by a significant increase in fluorescence, was obtained at a concentration of 10^{-7} M for both peptides (Figure 6E).

Penetration kinetics of fluorescein-conjugated hU-II and URP

Characterization of FL-hU-II and FL-URP translocation into living CHO-K1 cells revealed that the cellular uptake rate of both ligands was not significantly different (Figure 7A). After 10 min, about 41% (MFI: 31 ± 9) of the maximum FL-hU-II uptake (the maximal uptake of FL-hU-II or FL-URP being the MFI value obtained after 1 h of incubation with cells; MFI: 72 ± 6) had entered inside cells. After the same period of time, only 28% (MFI: 12 ± 3) of maximal FL-URP (MFI: 46 ± 10) was found in the cytoplasm (Figure 7A). This significant difference in cellular uptake, not uptake kinetics, between FL-hU-II and FL-URP was observed as soon as 2 min after the beginning of the experiment and up to the end. Moreover, using radiolabelled peptides (i.e. ^{125}I -hU-II and ^{125}I -URP) we were able to observe an efficient cellular uptake at a physiological concentration (0.2 nM) (Figure S5).

Influence of extracellular pH on cellular uptake of FL-hU-II and FL-URP

Following incubation of cells (CHO-K1) with FL-hU-II or FL-URP in media at different pH (6.5–8), cellular uptake

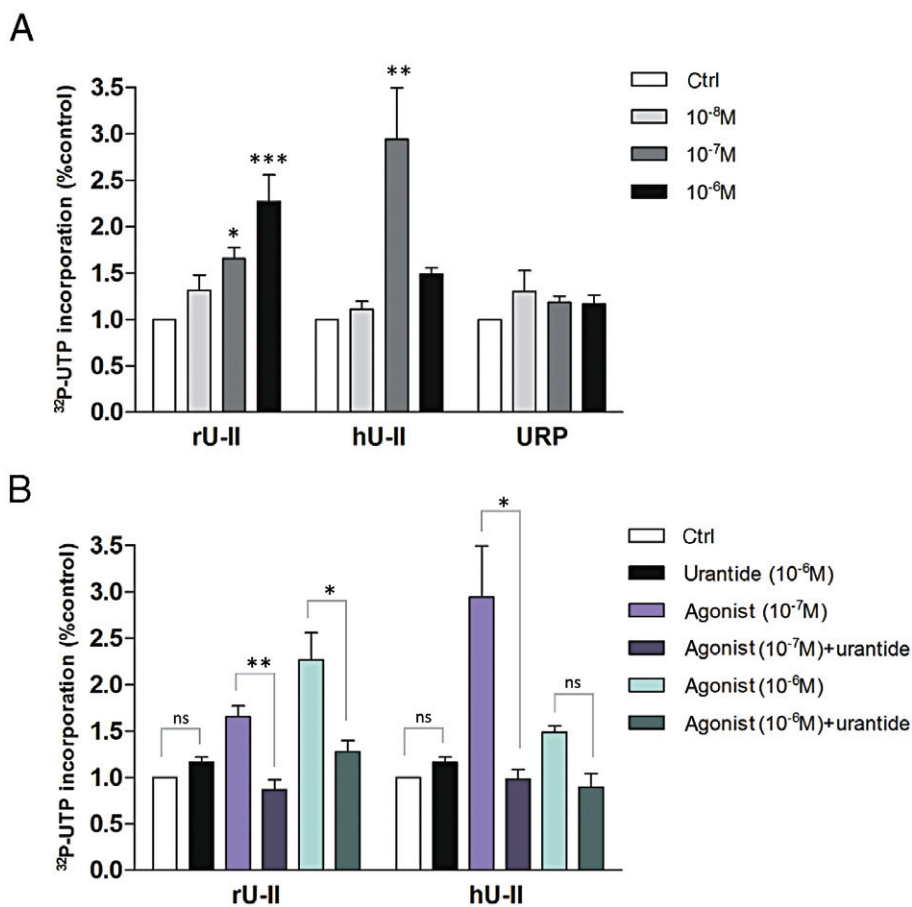


Figure 4

Regulation of UT transcriptional responses in nuclei isolated from rat heart. (A) Isolated nuclei were treated with increasing concentration of endogenous UT ligands (i.e. rat U-II, human U-II or URP). (B) Incorporation of [³²P]-UTP was measured in isolated nuclei either untreated or pretreated with UT-specific antagonist (i.e. urantide). Data, collected from at least three separate experiments, represent mean ± SEM. Significant differences (**P* < 0.05; ***P* < 0.01; ****P* < 0.001) were determined by one-way ANOVA followed by Dunnett's multiple comparison test or Student's unpaired *t*-test.

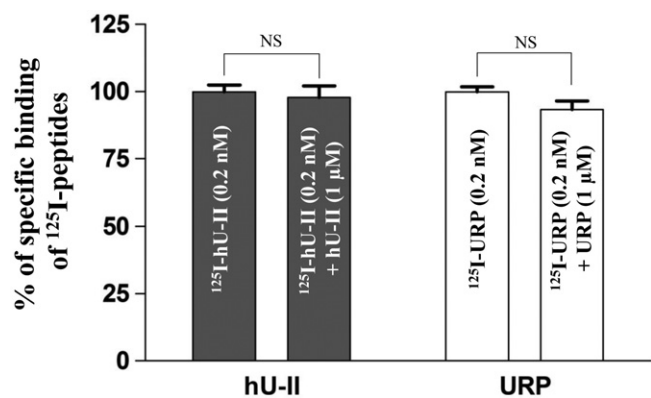


Figure 5

Displacement of bound [¹²⁵I]-hU-II or [¹²⁵I]-URP in CHO-K1 cells by hU-II or URP (10⁻⁶ M), respectively. Data are expressed as a percentage of the specific binding of [¹²⁵I]-hU-II or [¹²⁵I]-URP in the absence of the competitive ligands. Data represent the mean ± SEM of at least three independent assays performed in duplicate.

analysis was assessed by flow cytometry. Results showed no pH-dependent changes in the fluorescence signal of FL-URP, whereas at acidic pH (6.5), a significantly higher cellular uptake was recorded for the FL-hU-II-treated cells (Figure 7B). Noteworthy, at pH 6.5, but also at other pH values, the uptake of FL-hU-II compared to FL-URP was significantly higher. It should be noted that no difference in cell viability was observed (data not shown) in this experiment, and all cells positive for PI staining were excluded from the flow cytometry analysis.

Distinct uptake mechanism for hU-II and URP

As mentioned above, no specific U-II or URP binding sites were found on CHO-K1, HEK-293 or HeLa cells (Figure 5). Supporting these observations, pre-incubation of CHO-K1 cells with PTX, a G_{i/o}-protein inhibitor (0.2 μg·mL⁻¹, 6 h), did not affect the cellular uptake of either peptide (Figure 8A,C). Overall, these results suggest that both hU-II and URP can enter into cells by a receptor-independent mechanism such

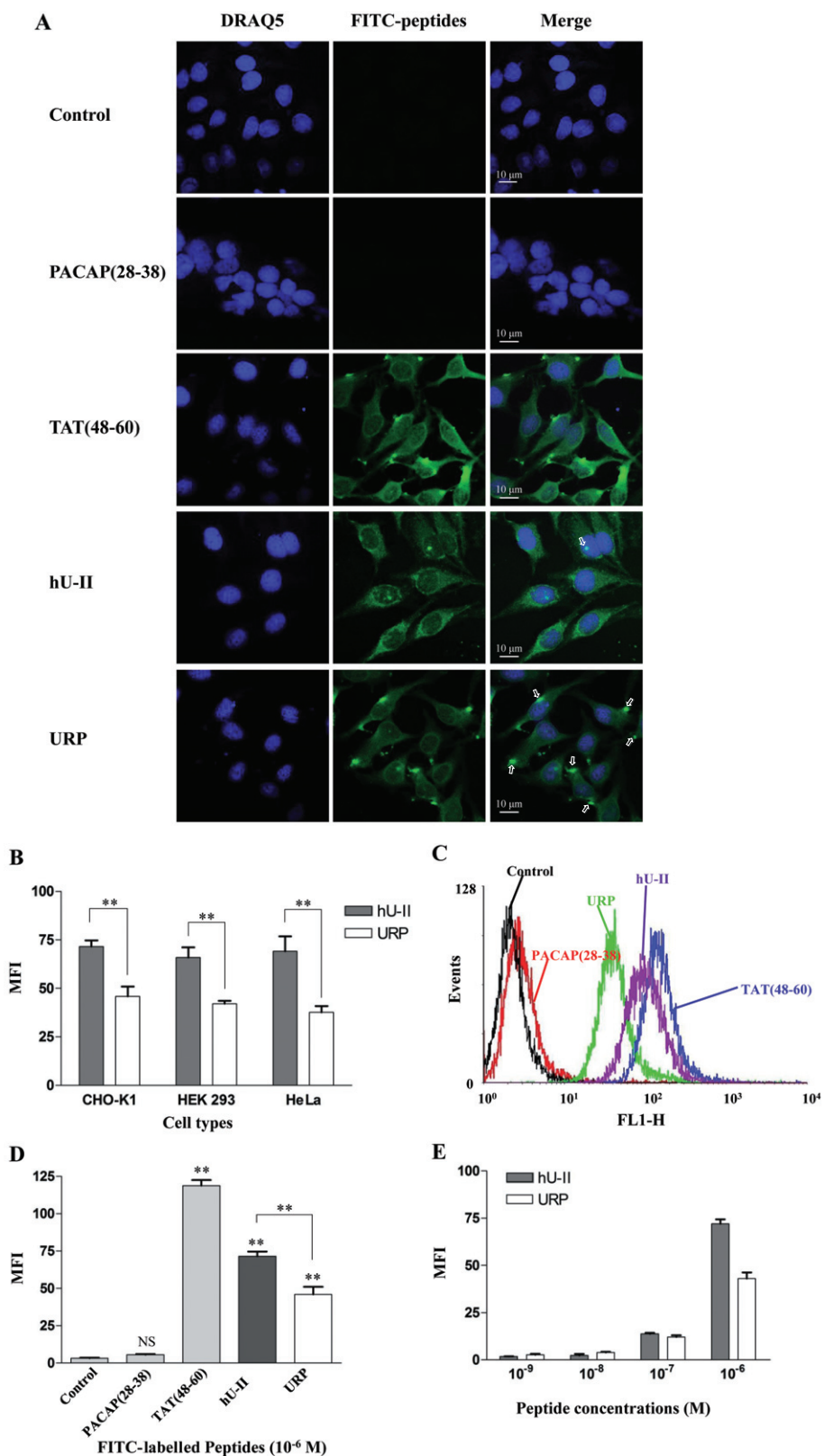


Figure 6

(A) Distribution of FITC-conjugated hU-II and URP in living untransfected CHO-K1 cells. Nuclei were stained with DRAQ5TM. In these experiments, FL-TAT(48–60) and FL-PACAP(28–38) were used as positive and negative control, respectively. (B) Cellular uptake efficiency of FL-hU-II and FL-URP in various cell lines. (C,D) Flow cytometry analysis of cell penetration of FL-hU-II, FL-URP, FL-PACAP(28–38) and FL-TAT(48–60) at a concentration of 10⁻⁶ M in CHO-K1 cells. (E) Effect of peptide concentration on cellular uptake. CHO-K1 cells were incubated with various concentrations of fluorescent peptides ranging from 10⁻⁹ to 10⁻⁶ M.

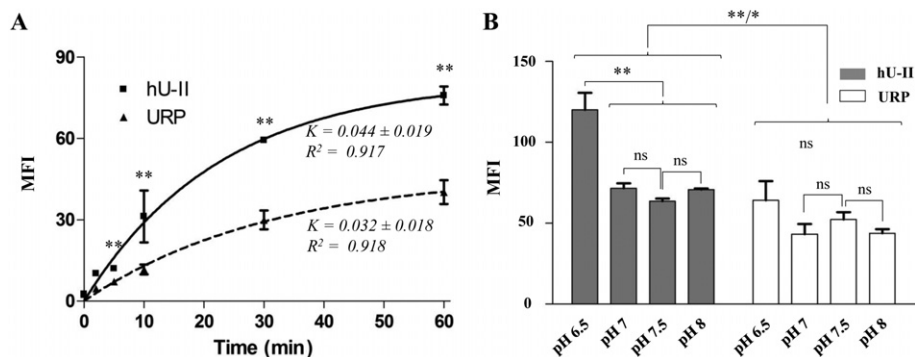


Figure 7

(A) Cellular uptake kinetics of FL-hU-II and FL-URP in CHO-K1 cells. CHO-K1 cells were incubated with FITC-conjugated peptides (10^{-6} M) for various periods of time. Maximal uptake was calculated as the amount of internalized peptide at 37°C after 1 h. (B) Effect of extracellular pH on the cellular uptake of FL-hU-II and FL-URP in CHO-K1 cells. Living cells were incubated for 1 h with fluorescent peptides (10^{-6} M) in HKR buffer for which the pH was adjusted at 6.5, 7.0, 7.5, and 8.0, respectively. Statistical significance was assessed by one-way or two-way ANOVA ($*P < 0.05$; $**P < 0.01$).

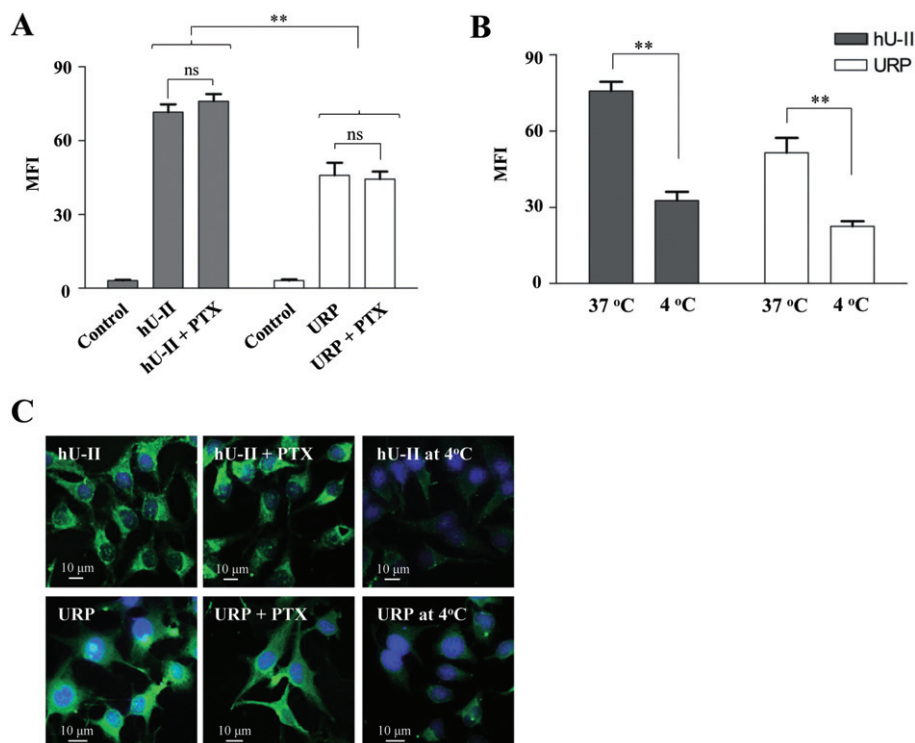


Figure 8

(A) Effect of pertussis toxin (PTX) on the cellular uptake of FL-hU-II or FL-URP in CHO-K1. PTX was added to cells placed in medium without FBS 6 h before addition of the fluorescent peptides (10^{-6} M). (B) Influence of low temperature on the cellular uptake of FL-hU-II or FL-URP in CHO-K1 cells. CHO-K1 cells were cooled to 4°C in serum-free medium for 15 min before a 1 h incubation with fluorescent peptides. (C) Confocal fluorescent images of the distribution of the fluorescent peptides following incubation with pertussis toxin or at low temperature.

as endocytosis, and/or direct translocation. Using confocal microscopy and flow cytometry experiments, after incubation of CHO-K1 cells at 4°C , we observed a significant reduction of the cellular uptake of both peptides (Figure 8B,C).

Cellular uptake of the peptides in the presence of NH_4Cl or chloroquine, known to inhibit endosomal acidification

and consequently slow endocytosis (Zaro *et al.*, 2009), was decreased, with the reduction being more severe for FL-URP ($27 \pm 3\%$ and $37 \pm 9\%$, respectively) than for FL-hU-II ($67 \pm 14\%$ and $76 \pm 10\%$, respectively) (Figure 9A,B).

Pretreatment of cells with amiloride (macropinocytosis inhibitor), nocodazole (a microtubule-disrupting reagent), maleimide (vesicular transport blocker) or hypertonic sucrose

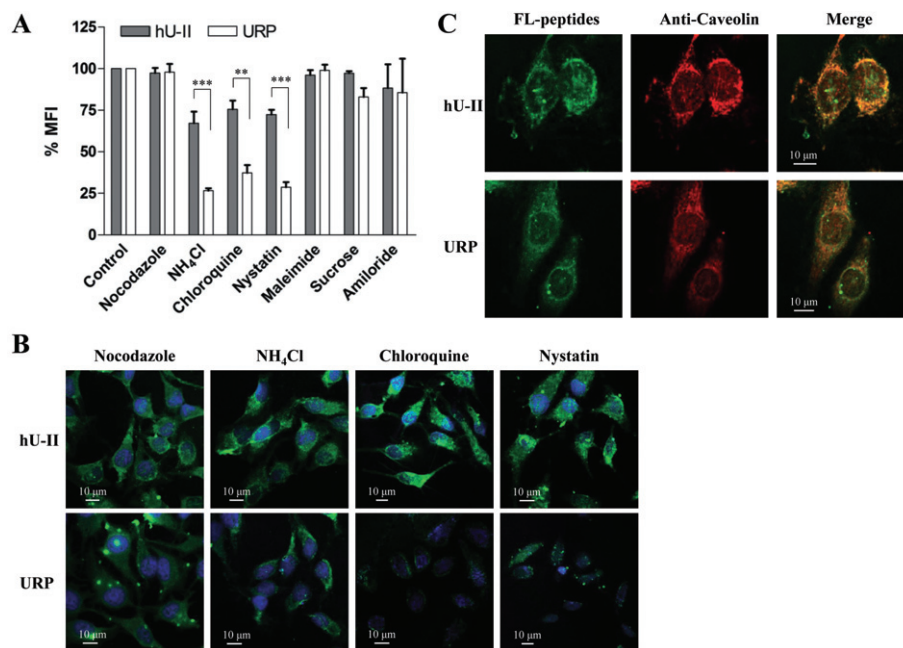


Figure 9

Effects of various endocytosis inhibitors on the cellular uptake of FL-hU-II and FL-URP in CHO-K1 cells. (A) For flow cytometry analysis, CHO-K1 cells were treated with different inhibitors as detailed in the Methods section. Values of MFI were normalized to that of the control experiments. Each point is the mean \pm SEM of three separate determinations. Statistical significance was assessed by ANOVA (** $P < 0.01$; *** $P < 0.001$). (B) Confocal fluorescent images of the distribution of the fluorescent peptides following treatment with endocytosis inhibitors. (C) Co-localization of hU-II or URP with caveolin in HeLa cells by confocal immunofluorescent microscopy. Cells were double-stained with FL-hU-II or FL-URP and anti-caveolin-3 as described in the Methods section.

(a blocker of clathrin-coated pits formation) had no significant effect on the cellular uptake of FL-hU-II or FL-URP (Figure 9A,B). Hence, it is unlikely that macropinocytosis or clathrin-mediated endocytosis are involved in the cellular uptake of FL-hU-II or FL-URP. However, pretreatment with nystatin, which binds cholesterol, disrupts lipid rafts along with caveolae structures and blocks caveolae function, significantly decreased the cellular uptake of FL-URP to $29 \pm 6\%$ (Figure 9A). Interestingly, FL-hU-II cellular uptake was less affected, suggesting that the hU-II uptake mechanism only partly involves a caveolin-dependent pathway. However, FL-hU-II and FL-URP were co-localized with caveolin-3 in the segregated caveolae compartment (Figure 9C). These results further indicate that, even though hU-II and URP share similar structural and physicochemical properties, they are translocated within the cell through different endocytic uptake mechanisms.

Discussion

By combining photolabelling experiments, Western blot analyses and radioligand binding assay, we were able to demonstrate the presence of the UT receptor in rat heart nuclear extracts. Interestingly, the presence of multiple immunoreactive spots in 2D-gel experiments was observed, which could be ascribed to either a single receptor subtype undergoing various forms of post-translational modification or multiple UT receptor isoforms simultaneously co-existing within cells

regardless of protein localization. Whether or not these patterns are involved in the variable U-II-associated biological activity will need further investigation. The presence of UT receptors in nuclei isolated from the cynomolgus monkey heart was demonstrated, suggesting that this particular pattern might also be found in other species including humans. Further, using characteristic proteins of specific cellular organelles, both nuclear preparations (i.e. rat and monkey heart nuclear extracts) were found to be free of membrane or mitochondrial contaminants. These results were supported by confocal microscopy that highlighted the presence of UT receptors in left ventricle heart tissue sections where it co-localized with lamin A, a protein related to the inner nuclear envelope. No immunostaining was observed in the right ventricle, suggesting the absence of UT receptors at both the membrane and the nuclei in this heart section. Such results have been observed previously in paraffin-embedded heart sections, where positive immunohistochemical staining was also observed in the left ventricle but not in the right ventricle and atria (Gong *et al.*, 2004). A perinuclear localization of the rat UT receptor was reported in UT-transfected HEK-293 cells in the absence of stimulation by its cognate ligand (Giebing *et al.*, 2005). Several vasoactive GPCRs, including endothelin, angiotensin and β -adrenoceptors, have been shown to be present in the nuclear/perinuclear environment (Boivin *et al.*, 2008). These intracellular receptors may have the capacity to regulate signalling pathways that differ from those of their plasma membrane counterparts, as recently demonstrated for the metabotropic glutamate recep-

tor 5 (Jong *et al.*, 2009) and the renin–angiotensin system (De Mello, 2008). In this study, we observed that U-II and URP, both endogenous ligands of UT, have very distinct roles as regards transcription initiation. Rat U-II dose-dependently increased transcriptional activity, whereas the observed effect of hU-II on [³²P]-UTP incorporation was biphasic. Rat U-II and hU-II differ in their composition and the length of their respective N-terminal segments (Vaudry *et al.*, 2010). Although it has been reported that this section is not mandatory for full biological activity (Leprince *et al.*, 2008), it might interact in a specific manner with the receptor, changing its conformation and therefore triggering complementary signalling. Further, rat and human UT receptors share around 75% of sequence homology (Elshourbagy *et al.*, 2002). Thus, a possible explanation for the observed effect could be an impaired interaction of the N-terminal domain of hU-II with the rat UT receptor, leading to a rapid desensitization of the receptor. Even though it was previously demonstrated that hU-II induces chemotaxis of peripheral human blood mononuclear cells (Segain *et al.*, 2007) and plasma extravasation in mice (Vergura *et al.*, 2004) with a typical bell-shaped dose–response curve associated with a receptor-mediated effect, further experiments are needed to clarify the difference between hU-II and rU-II.

There is no doubt that U-II and URP are endogenous agonists of UT (Vaudry *et al.*, 2010). Surprisingly, URP had no effect with regards to transcription initiation. Signalling pathways associated with UT activation have been studied, but mostly in relation to U-II and not URP as U-II was discovered almost 10 years before URP, and because both peptides have similar affinity on transfected cells system and potency on rat aortic ring (Vaudry *et al.*, 2010). The main transduction pathway associated with UT activation by U-II involves the recruitment of Gαq/11, Gαi/o, and G_{12/13} subtypes of G-proteins with a subsequent increase in inositol triphosphates (IP₃) (Proulx *et al.*, 2008), ERK1/2 and RhoA activation (Guidolin *et al.*, 2010). However, recent studies have demonstrated that U-II and URP regulate astrocyte activity (Jarry *et al.*, 2010) and cardiac contractility (Prosser *et al.*, 2008) differently. Thus, it is conceivable that U-II, which structurally differs from URP due to the presence of an extended N-terminal domain that varies in length and composition, might induce a different conformational change in UT upon binding and activation. Involvement of the N-terminal peptide region in the differences in biological activity between U-II and URP has already been suggested (Prosser *et al.*, 2008). Hence, as U-II and URP share common functions, the concept of URP being an endogenous biased agonist of the urotensinergic system is proposed. The concept of biased agonist has recently emerged from various studies, resulting in the hypothesis that specific ligand-induced conformational changes can lead to precisely directed signalling (Patel *et al.*, 2010). It is thus conceivable that a similar pattern is taking place, and that hU-II and URP are able to trigger not only common but also different second messengers, leading to divergent physiological actions.

As mentioned earlier, the nuclear preparation used in this experiment is devoid of membrane or mitochondrial contaminants. Further, as exemplified in a previous report (Boivin *et al.*, 2003), the protocol used for heart nuclei isolation results in the presence of negligible amounts of endo-

plasmic reticulum elements. Therefore, the observed effect on transcriptional activity can definitely be ascribed to nuclear activity. It is well established that cell calcium signalling affects nuclear activity, and that the amplitude and frequency of global cellular calcium can regulate gene transcription (Dolmetsch *et al.*, 1998). The machinery required for the generation of calcium mobilizing messengers, such as the ADP-ribosyl cyclase enzyme and phosphoinositide-specific PLC, exists in nuclei (Bootman *et al.*, 2009). Moreover, it has been shown that nuclei possess phosphoinositide signalling mechanisms that lead to IP₃ production (Ye and Ahn, 2008). Interestingly, UT-mediated calcium mobilization has been linked to IP₃ production and Gq activation (Jarry *et al.*, 2010). Thus, in a similar fashion to the signalling taking place at the plasma membrane, activation of the UT receptor found on isolated nuclei could be associated with phosphoinositide activation, leading to the accumulation of calcium in nucleoplasm. Noteworthy, such nuclear calcium signals have been shown to stimulate gene transcription following nuclear angiotensin receptor activation in isolated cardiomyocytes (Tadevosyan *et al.*, 2010). Overall, these observations, which support a physiological and/or pathophysiological role for nuclear GPCRs, suggest that nuclear UT receptors might represent new or complementary therapeutic targets that should be taken into account during drug development.

A key question still remains regarding how these intracellular UT receptors are activated by their endogenous ligands. In this study, FITC-conjugated hU-II and URP were both able to reach the internal cell compartment through receptor-independent mediated endocytosis in cell lines not expressing the UT receptor. However, higher levels of FL-hU-II were found in the cytoplasm compared to FL-URP. Because the only difference found between hU-II and URP is in the sequence and length of the N-terminal region, the higher propensity of hU-II compared to URP to cross the plasma membrane might be ascribed to the specific physicochemical characteristics of this domain. Pretreatment of the cell with ammonium chloride or chloroquine, known to reduce the acidification of the endosome–lysosome system and consequently slow endocytosis, only dramatically reduced the cellular uptake of URP, characterized by a punctuate cytoplasmic distribution. These results suggest that URP, and to a lesser extent hU-II, might be trapped inside endocytic vesicles. Moreover, the fact that hU-II is less sensitive to ammonium chloride and chloroquine pretreatment suggests that hU-II can also escape more efficiently from the endosomal/lysosomal compartments. In addition, MALDI-TOF analysis of cell lysates, incubated for 1 h with native peptides, revealed that the integrity of hU-II and URP, at least in terms of amino acid sequence, is conserved, indicating that they might be stable enough in the cytoplasm to activate the intracellular receptor (data not shown). In a cell system, co-expressing membrane and nuclear receptors, the receptor-mediated endocytosis might be complemented by the receptor-independent translocation we describe in this study. Following internalization of peptide–receptor complexes, acidification of the endosome will induce dissociation of complexes and recycling of the receptor to the outer membrane (Giebing *et al.*, 2005). In this particular case, the fate of the peptide is not known, but based on our results, we assume that it might be able to leak from the vesicle and ultimately

activate the intracellular receptor. Also, the intracellular production of U-II and/or URP, as demonstrated for the angiotensin system (Singh *et al.*, 2007), is another possibility to be considered. To this extent, it is worth mentioning that the human U-II precursor is synthesized as two isoforms differing only in their peptide signal (Coulouarn *et al.*, 1998; Ames *et al.*, 1999). Comparison of peptide signal amino acid composition revealed a poor sequence homology that might reflect the fact that one sequence contains a specific signal associated with trafficking to the nuclei, as demonstrated recently for the pituitary adenylate cyclase-activating polypeptide (PACAP) gene (Tominaga *et al.*, 2010). Altogether, these observations indicate that hU-II, but not URP, is a potential intracrine factor.

The demonstrated ability of hU-II and URP to cross the plasma membrane, by a receptor-independent endocytic mechanism including the caveolin-dependent pathway, has provided new insights into the pseudo-irreversible binding characteristics often described. The inability to desensitize UT through classic mechanisms (acid wash or trypsin treatments) was thought to reflect the strong, pseudo-irreversible nature of U-II binding (Douglas and Ohlstein, 2000). Based on our results, it is conceivable that part of the pseudo-irreversible character is due to the ability of both endogenous peptides to translocate within the internal compartment of the cell. To support this hypothesis, Castel and colleagues demonstrated that temperature reduction affected the irreversible nature of the binding (Castel *et al.*, 2006). In the same way, the pseudo-irreversibility, as well as the slow internalization process of UT receptors (half-life: 15 min) account for the unusual sustained cellular responses, leading to potent vasoconstriction (Douglas and Ohlstein, 2000; Giebing *et al.*, 2005; Du *et al.*, 2010). However, it is well established that intracrine factors can form intracellular positive feedback loops, thereby maintaining a specific cellular state (Petersen *et al.*, 2006).

Identification of the precise role of this new intracellular urotensinergic system will need further experiments especially in order to ascertain if the two systems work in synergy or independently of each other. U-II and its receptor were found to be up-regulated in the failing heart (Nakayama *et al.*, 2008). In addition, elevated plasma levels of U-II have been demonstrated in numerous disease conditions, including hypertension, atherosclerosis, heart failure, pulmonary hypertension, diabetes, renal failure and the metabolic syndrome (Ross *et al.*, 2010). As observed, hU-II and URP are both able to efficiently enter the cell, this uptake being increased for hU-II at lower pH. Many pathological conditions, such as cancer, ischaemic stroke, inflammation and atherosclerotic plaques, are associated with increased metabolic activity and hypoxia resulting in an elevated extracellular acidity (Andreev *et al.*, 2010). For instance, the contractility of heart muscle is sensitive to small, physiological changes in the extracellular pH. A reduction in contractility associated with acidosis has been involved in a number of pathological conditions, most dramatically during myocardial ischaemia (Crampin *et al.*, 2006). Therefore, in such conditions where U-II is able to enter the cell more easily than URP, specific gene transcription associated with U-II activation of the nuclear receptor will be triggered. In fact, isolated ischaemic heart experiments revealed that both U-II and URP

are able to decrease myocardial damage by reducing creatine kinase, but only U-II reduced atrial natriuretic peptide (ANP) production, and hence blocked the production of VEGF and inhibited angiogenesis (Prosser *et al.*, 2008). Thus, following a decrease in membrane pH during hypoxic conditions, it is reasonable to assume that the inhibition of ANP production by hU-II might be the result of the nuclear receptor activation.

In conclusion, we report here, for the first time, a specific nuclear/perinuclear expression of the U-II receptor in the rat and monkey heart, which upon activation by U-II or URP results in different modulatory effects on transcription. Although the physiological role of this nuclear GPCR remains to be established, our results suggest that nuclear UT receptors are associated with a specific biological role and that U-II, which is able to specifically activate nuclear UT receptors, but not URP, should be considered as an intracrine factor. This study also highlighted a complementary receptor-independent mediated endocytosis that might be, at least in part, involved in the intracellular presence of UT ligands. Most antagonists developed so far have failed in clinical trials for several reasons including a lack of efficacy in pathological *in vivo* models, low potency, low selectivity or concomitant agonist/antagonist behaviour (Maryanoff and Kinney, 2010). However, the lack of efficacy of such compounds might also be related to their inability to reach and block the action of the nuclear UT receptor. Critical questions still remain such as 'Are the pleiotropic effects within the cardiovascular system, including modulation of cardiac contractility, vascular tone, cell proliferation and cell growth, equally modulated by U-II and URP?' and 'Are these actions directly associated with the activation of the nuclear and/or the membrane receptor?' Nevertheless, the presence of functional UT receptors at the cell membrane and at the nucleus should be taken into account during the development of new therapeutic compounds for the treatment of pathologies associated with the urotensinergic system.

Acknowledgements

This work was supported by the Canadian Institutes of Health Research. NDD is the recipient of a studentship from the Heart and Stroke Foundation of Canada and the Fondation Armand-Frappier. TTMN and KT are recipients of a studentship from Fondation Armand-Frappier.

Conflicts of interest

None.

References

- Ames RS, Sarau HM, Chambers JK, Willette RN, Aiyar NV, Romanic AM *et al.* (1999). Human urotensin-II is a potent vasoconstrictor and agonist for the orphan receptor GPR14. *Nature* 401: 282–286.

- Andreev OA, Karabadzahk AG, Weerakkody D, Andreev GO, Engelman DM, Reshetnyak YK (2010). pH (low) insertion peptide (pHLIP) inserts across a lipid bilayer as a helix and exits by a different path. *Proc Natl Acad Sci U S A* 107: 4081–4086.
- Boivin B, Chevalier D, Villeneuve LR, Rousseau E, Allen BG (2003). Functional endothelin receptors are present on nuclei in cardiac ventricular myocytes. *J Biol Chem* 278: 29153–29163.
- Boivin B, Lavoie C, Vaniotis G, Baragli A, Villeneuve LR, Ethier N *et al.* (2006). Functional beta-adrenergic receptor signalling on nuclear membranes in adult rat and mouse ventricular cardiomyocytes. *Cardiovasc Res* 71: 69–78.
- Boivin B, Vaniotis G, Allen BG, Hebert TE (2008). G protein-coupled receptors in and on the cell nucleus: a new signaling paradigm? *J Recept Signal Transduct Res* 28: 15–28.
- Bootman MD, Fearnley C, Smyrniak I, MacDonald F, Roderick HL (2009). An update on nuclear calcium signalling. *J Cell Sci* 122 (Pt 14): 2337–2350.
- Brkovic A, Hattenberger A, Kostenis E, Klabunde T, Flohr S, Kurz M *et al.* (2003). Functional and binding characterizations of urotensin II-related peptides in human and rat urotensin II-receptor assay. *J Pharmacol Exp Ther* 306: 1200–1209.
- Castel H, Diallo M, Chatenet D, Leprince J, Desrues L, Schouff MT *et al.* (2006). Biochemical and functional characterization of high-affinity urotensin II receptors in rat cortical astrocytes. *J Neurochem* 99: 582–595.
- Chatenet D, Dubessy C, Leprince J, Boullaran C, Carlier L, Segalas-Milazzo I *et al.* (2004). Structure-activity relationships and structural conformation of a novel urotensin II-related peptide. *Peptides* 25: 1819–1830.
- Coulouarn Y, Lihmann I, Jegou S, Anouar Y, Tostivint H, Beauvillain JC *et al.* (1998). Cloning of the cDNA encoding the urotensin II precursor in frog and human reveals intense expression of the urotensin II gene in motoneurons of the spinal cord. *Proc Natl Acad Sci U S A* 95: 15803–15808.
- Crampin EJ, Smith NP, Langham AE, Clayton RH, Orchard CH (2006). Acidosis in models of cardiac ventricular myocytes. *Philos Transact A Math Phys Eng Sci* 364: 1171–1186.
- De Mello WC (2008). Intracellular and extracellular renin have opposite effects on the regulation of heart cell volume. Implications for myocardial ischaemia. *J Renin Angiotensin Aldosterone Syst* 9: 112–118.
- Dennison SR, Baker RD, Nicholl ID, Phoenix DA (2007). Interactions of cell penetrating peptide Tat with model membranes: a biophysical study. *Biochem Biophys Res Commun* 363: 178–182.
- Doan ND, Bourgault S, Dejda A, Letourneau M, Detheux M, Vaudry D *et al.* (2011). Design and in vitro characterization of PAC1/VPAC1-selective agonists with potent neuroprotective effects. *Biochem Pharmacol* 81: 552–561.
- Dolmetsch RE, Xu K, Lewis RS (1998). Calcium oscillations increase the efficiency and specificity of gene expression. *Nature* 392: 933–936.
- Douglas SA, Ohlstein EH (2000). Human urotensin-II, the most potent mammalian vasoconstrictor identified to date, as a therapeutic target for the management of cardiovascular disease. *Trends Cardiovasc Med* 10: 229–237.
- Du AT, Onan D, Dinh DT, Lew MJ, Ziogas J, Aguilar MI *et al.* (2010). Ligand-supported purification of the urotensin-II receptor. *Mol Pharmacol* 78: 639–647.
- Dubessy C, Cartier D, Lectez B, Buchares C, Chartrel N, Montero-Hadjadje M *et al.* (2008). Characterization of urotensin II, distribution of urotensin II, urotensin II-related peptide and UT receptor mRNAs in mouse: evidence of urotensin II at the neuromuscular junction. *J Neurochem* 107: 361–374.
- Elshourbagy NA, Douglas SA, Shabon U, Harrison S, Duddy G, Sechler JL *et al.* (2002). Molecular and pharmacological characterization of genes encoding urotensin-II peptides and their cognate G-protein-coupled receptors from the mouse and monkey. *Br J Pharmacol* 136: 9–22.
- Erchevyi J, Hoeger CA, Low W, Hoyer D, Waser B, Eltschinger V *et al.* (2005). Somatostatin receptor 1 selective analogues: 2. N(alpha)-Methylated scan. *J Med Chem* 48: 507–514.
- Ferone D, Boschetti M, Resmini E, Giusti M, Albanese V, Goglia U *et al.* (2006). Neuroendocrine-immune interactions: the role of cortistatin/somatostatin system. *Ann N Y Acad Sci* 1069: 129–144.
- Giebing G, Tolle M, Jurgensen J, Eichhorst J, Furkert J, Beyermann M *et al.* (2005). Arrestin-independent internalization and recycling of the urotensin receptor contribute to long-lasting urotensin II-mediated vasoconstriction. *Circ Res* 97: 707–715.
- Gong H, Wang YX, Zhu YZ, Wang WW, Wang MJ, Yao T *et al.* (2004). Cellular distribution of GPR14 and the positive inotropic role of urotensin II in the myocardium in adult rat. *J Appl Physiol* 97: 2228–2235.
- Guidolin D, Albertin G, Oselladore B, Sorato E, Rebuffat P, Mascarini A *et al.* (2010). The pro-angiogenic activity of urotensin-II on human vascular endothelial cells involves ERK1/2 and PI3K signaling pathways. *Regul Pept* 162: 26–32.
- Holm T, Johansson H, Lundberg P, Pooga M, Lindgren M, Langel U (2006). Studying the uptake of cell-penetrating peptides. *Nat Protoc* 1: 1001–1005.
- Jarry M, Diallo M, Lecointre C, Desrues L, Tokay T, Chatenet D *et al.* (2010). The vasoactive peptides urotensin II and urotensin II-related peptide regulate astrocyte activity through common and distinct mechanisms: involvement in cell proliferation. *Biochem J* 428: 113–124.
- Jong YJ, Kumar V, O'Malley KL (2009). Intracellular metabotropic glutamate receptor 5 (mGluR5) activates signaling cascades distinct from cell surface counterparts. *J Biol Chem* 284: 35827–35838.
- Jullian M, Hernandez A, Maurras A, Puget K, Amblard M, Martinez J *et al.* (2009). N-terminus FITC labeling of peptides on solid support: the truth behind the spacer. *Tetrahedron Lett* 50: 260–263.
- Lavecchia A, Cosconati S, Novellino E (2005). Architecture of the human urotensin II receptor: comparison of the binding domains of peptide and non-peptide urotensin II agonists. *J Med Chem* 48: 2480–2492.
- Leprince J, Chatenet D, Dubessy C, Fournier A, Pfeiffer B, Scalbert E *et al.* (2008). Structure-activity relationships of urotensin II and URP. *Peptides* 29: 658–673.
- Maryanoff BE, Kinney WA (2010). Urotensin-II receptor modulators as potential drugs. *J Med Chem* 53: 2695–2708.
- Nakayama T, Hirose T, Totsune K, Mori N, Maruyama Y, Maejima T *et al.* (2008). Increased gene expression of urotensin II-related peptide in the hearts of rats with congestive heart failure. *Peptides* 29: 801–808.
- Patel CB, Noor N, Rockman HA (2010). Functional selectivity in adrenergic and angiotensin signaling systems. *Mol Pharmacol* 78: 983–992.

Petersen MC, Munzenmaier DH, Greene AS (2006). Angiotensin II infusion restores stimulated angiogenesis in the skeletal muscle of rats on a high-salt diet. *Am J Physiol Heart Circ Physiol* 291: H114–H120.

Prosser HC, Forster ME, Richards AM, Pemberton CJ (2008). Urotensin II and urotensin II-related peptide (URP) in cardiac ischemia-reperfusion injury. *Peptides* 29: 770–777.

Proulx CD, Holleran BJ, Lavigne P, Escher E, Guillemette G, Leduc R (2008). Biological properties and functional determinants of the urotensin II receptor. *Peptides* 29: 691–699.

Ross B, McKendy K, Giaid A (2010). Role of urotensin II in health and disease. *Am J Physiol Regul Integr Comp Physiol* 298: R1156–R1172.

Russell FD (2008). Urotensin II in cardiovascular regulation. *Vasc Health Risk Manag* 4: 775–785.

Segain JP, Rolli-Derkinderen M, Gervois N, Raingard de la Bletiere D, Loirand G, Pacaud P (2007). Urotensin II is a new chemotactic factor for UT receptor-expressing monocytes. *J Immunol* 179: 901–909.

Singh VP, Le B, Bhat VB, Baker KM, Kumar R (2007). High-glucose-induced regulation of intracellular ANG II synthesis and nuclear redistribution in cardiac myocytes. *Am J Physiol Heart Circ Physiol* 293: H939–H948.

Sugo T, Mori M (2008). Another ligand fishing for G protein-coupled receptor 14. Discovery of urotensin II-related peptide in the rat brain. *Peptides* 29: 809–812.

Tadevosyan A, Maguy A, Villeneuve LR, Babin J, Bonnefoy A, Allen BG *et al.* (2010). Nuclear-delimited angiotensin receptor-mediated signaling regulates cardiomyocyte gene expression. *J Biol Chem* 285: 22338–22349.

Tominaga A, Sugawara H, Futagawa T, Inoue K, Sasaki K, Minamino N *et al.* (2010). Characterization of the testis-specific promoter region in the human pituitary adenylate cyclase-activating polypeptide (PACAP) gene. *Genes Cells* 15: 595–606.

Tostivint H, Lihmann I, Vaudry H (2008). New insight into the molecular evolution of the somatostatin family. *Mol Cell Endocrinol* 286: 5–17.

Vaniotis G, Del Duca D, Trieu P, Rohlicek CV, Hebert TE, Allen BG (2011). Nuclear beta-adrenergic receptors modulate gene expression in adult rat heart. *Cell Signal* 23: 89–98.

Vaudry H, Do Rego JC, Le Mevel JC, Chatenet D, Tostivint H, Fournier A *et al.* (2010). Urotensin II, from fish to human. *Ann N Y Acad Sci* 1200: 53–66.

Vergura R, Camarda V, Rizzi A, Spagnol M, Guerrini R, Calo G *et al.* (2004). Urotensin II stimulates plasma extravasation in mice via UT receptor activation. *Naunyn Schmiedebergs Arch Pharmacol* 370: 347–352.

Ye K, Ahn JY (2008). Nuclear phosphoinositide signaling. *Front Biosci* 13: 540–548.

Zaro JL, Vekich JE, Tran T, Shen WC (2009). Nuclear localization of cell-penetrating peptides is dependent on endocytosis rather than cytosolic delivery in CHO cells. *Mol Pharm* 6: 337–344.

Supporting information

Additional Supporting Information may be found in the online version of this article:

Figure S1 (A) Amino acid sequence of synthesized peptides. (B) Analytical data obtained by MALDI-TOF spectrometry and by RP-HPLC. ^aPercentage of purity determined by HPLC using a buffer system [A = H₂O (pH 2.5) and B = 100% CH₃CN] with a gradient slope of 1% B per minute, at a flow rate of 1 mL·min⁻¹ on a Vydac C₁₈ column (5 μm particle size, 300 Å pore size). Detection at 214 nm. ^bObserved *m/z*-value compared with the calculated [M + H]⁺ monoisotopic mass. (C) Effect of hU-II or N-biotin-[Ahx⁰, Bpa³]-hU-II on Ca²⁺ mobilization using CHO cells co-expressing human UT receptors and a mitochondrial apo-aequorin protein. Data are expressed as a percentage of the response (bioluminescence) obtained with digitonin (50 μM) added to the same 96-well culture plate. Data represent the mean ± SEM of at least four independent assays performed in duplicate.

Figure S2 Enlargement of a nucleus from Figure 4D. Nucleus was stained with DRAQ5TM (blue colour). Left ventricular sections are double-stained for lamin A (red colour) and UT (green colour). This enlargement demonstrates the co-localization of UT (yellow colour, arrowhead) and lamin A.

Figure S3 Distribution of FITC-conjugated hU-II and URP in fixed untransfected CHO-K1 cells. Nuclei were stained with PI.

Figure S4 Distribution of FITC-conjugated hU-II and URP in living (A) HeLa and (B) HEK-293 cells. Nuclei were stained with DRAQ5TM.

Figure S5 Internalization of ¹²⁵I-hU-II and ¹²⁵I-URP in CHO-K1 cells. CHO-K1 cells in 12-well plates were incubated for various periods of time in FBS-free media containing 0.2 nM ¹²⁵I-hU-II or ¹²⁵I-URP. Internalization was stopped by washing, and cells were then solubilized with 1 M NaOH, and the radioactivity was quantified using a γ-counter. Membrane-bound radioactivity was evaluated by incubation of CHO-K1 cells with ¹²⁵I-labelled peptide (0.05 nM) for 30 s. **Appendix S1** Methods.

Please note: Wiley-Blackwell are not responsible for the content or functionality of any supporting materials supplied by the authors. Any queries (other than missing material) should be directed to the corresponding author for the article.